Journal of Energetic Materials
Publication details, including instructions for authors and subscription information:
http://www.informaworld.com/smpp/title~content=t713770432

Characterization and Thermal Analysis of Hydrazinium Nitroformate (HNF)

P. S. Dendage; D. B. Sarwade; A. B. Mandale; S. N. Asthana

To cite this Article Dendage, P. S. , Sarwade, D. B. , Mandale, A. B. and Asthana, S. N.(2003) 'Characterization and Thermal Analysis of Hydrazinium Nitroformate (HNF)', Journal of Energetic Materials, 21: 3, 167 — 183
To link to this Article: DOI: 10.1080/716100384
URL: http://dx.doi.org/10.1080/716100384

Energetic Materials, 21: 167–183, 2003

ISSN: 0737-0652 print
DOI: 10.1080/07370650390256647

Taylor & Francis
Taylor & Francis Group

Characterization and Thermal Analysis of Hydrazinium Nitroformate (HNF)

P. S. DENDAGE
D. B. SARWADE
A. B. MANDALE

High Energy Materials Research Laboratory
Sutarwadi, Pune, India

S. N. ASTHANA

National Chemical Laboratory
Pashan, Pune, India

This paper reports studies undertaken on hydrazinium nitroformate (HNF) synthesized in HEMRL by a viable method. The purity of the synthesized HNF was determined by high-performance liquid chromatography, and the compound was characterized by elemental analysis, ultraviolet, infrared, nuclear magnetic resonance (^{1}H NMR and ^{13}C NMR), and electron impact mass spectroscopy.

Detailed studies on the crystallographic nature and surface chemistry of HNF were undertaken by applying scanning electron microscopy (SEM), X-ray diffraction (XRD), transmission electron microscopy (TEM), and X-ray photo-electron spectroscopy (XPS). SEM shows layered needle-shaped crystals of HNF. The d values obtained in XRD spectra establish monoclinic structure, as reported by other investigators. TEM provides confirmatory data. The XPS study offers additional information regarding the surface chemistry of HNF. The evidence is in favor of intermolecular hydrogen bonding to a large extent.

Address correspondence to P. S. Dendage, High Energy Materials Research Laboratory, Sutarwadi Pune 411021, India. E-mail: kdendage@vsnl.com

Thermal studies were also conducted as part of this work. Differential thermal analysis, thermogravimetry, and differential scanning calorimetry results reveal two-stage decomposition of HNF. DSC results correspond to the activation energy of ∼150 kJ/mol for both the stages of decomposition.

1. Introduction

Superior energy potential combined with eco-friendly nature of the solid oxidizer are vital requirements of futuristic solid rocket propellants. In the present global scenario, ammonium dinitramide (ADN) and hydrazinium nitroformate (HNF) are emerging as likely substitutes to ammonium perchlorate (AP) [1,2]. ADN has processing and storage problems due to its hygroscopic nature. Its other limitation is a low melting point (<100°C). On the other hand, HNF is nonhygroscopic in nature and has a melting point above 100°C. Moreover, its synthesis is comparatively simple. Purity levels of HNF have bearing on its sensitivity and stability [3,4] . Quality of chemicals, solvents, stoichometric ratio of reactants and reaction parameters play an important role in deciding the purity of HNF [1,6,7]. Needle-shaped crystals of HNF with high L/D ratio pose loading problem in solid propellant compositions [1]. The desired morphology of HNF is the critical requirement from the processing point of view.

This paper discusses work carried out on synthesis, characterization, and thermal decomposition of HNF in this laboratory. In view of the increasing importance of HNF as an energetic and eco-friendly oxidizer, research institutes all over the globe have undertaken programs to synthesize and produce HNF. Different synthesis approaches have been adopted, resulting in different purity levels and dissimilar morphology of HNF.

The present work was undertaken to generate data on HNF synthesized in HEMRL and correlate it with reported literature. The main feature of this work is extensive investigation on crystallography and the surface chemistry of HNF by applying transmission electron microscopy (TEM) and X-ray photo-electron spectroscopy (XPS) in addition to scanning electron microscopy (SEM) and X-ray diffraction (XRD). In an attempt to understand the thermal behavior, HNF was subjected to hyphenated TG-FTIR analysis in addition to differential thermal analysis (DTA), differential scanning calorimetry (DSC), and thermogravimetry (TG).

2. Experimental

HNF synthesis was carried out using fuming nitric acid (conc.>95%), sulphuric acid, iso-propanol, ethylene dichloride, and hydrazine hydrate of AR grade. The purity was determined by high-performance liquid chromatography (HPLC) with micro-C18 column. The compound was characterized by elemental analysis and ultraviolet (UV) and infrared (IR) spectroscopy. ^{1}H NMR and ^{13}C NMR spectra were recorded using TMS as internal standard. The sample was also analyzed by an electron impact mass spectrum (EIMS) with a 70 eV direct insertion probe.

Morphology of HNF was studied by SEM, XRD, and TEM spectrometry. The X-ray photo electron spectroscope (XPS) study was carried out on the ESCA-3000 instrument with 1.6 eV resolution.

Non-isothermal TG/DTA curves were recorded in static air at 10°C/min heating rate. DSC curves were recorded at the heating rates of 5–25°C/min in N_2 atmosphere. Activation energy (E) was computed by applying Kissinger [8] (1) and Ozawa [9] (2) equations for both exotherms:

$$\frac{E\beta}{RT_m} = An(1-x)_m{}^{n-1} e^{-E/RTm}, \tag{1}$$

$$\log\beta = 0.4567\,\frac{E}{RT_m}, \tag{2}$$

where,

E = activation energy
A = frequency factor
β = heating rate
n = order of reaction
T_m = peak temperature (K)
R = universal gas constant
$(1-x)_m$ = fraction of unreacted material at T_m.

E is calculated from the slope of the plot of β/RT_m Versus $1/T_m$ for the Kissinger method and log β Versus $1/T_m$ for the Ozawa method.

3. Results and discussion

3.1 Synthesis and Characterization of HNF

During this work nitroform (NF) was synthesized by nitration of isopropano [10]. It was isolated from the acid impurities by the extraction

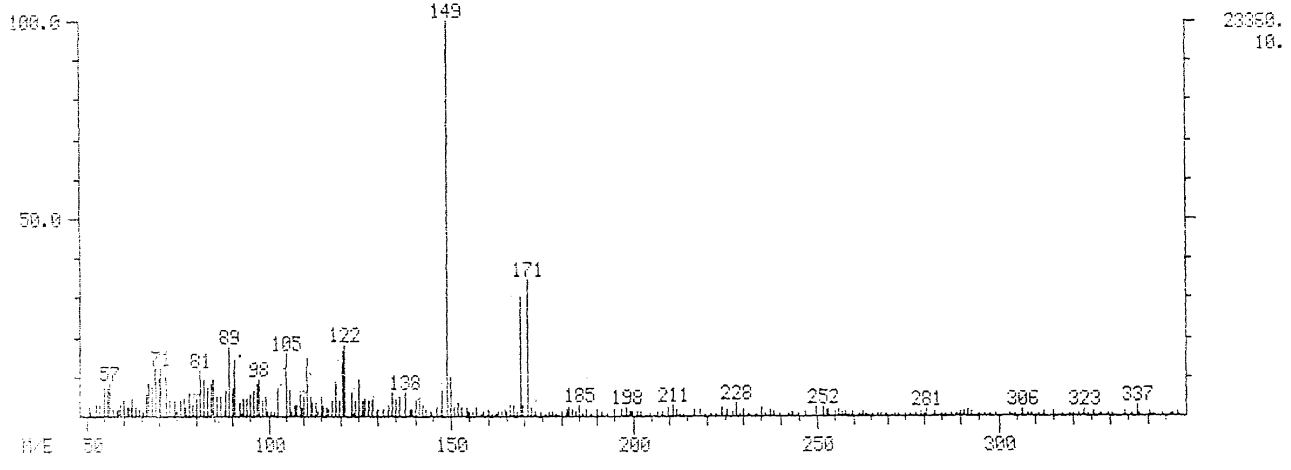

Figure 1. Mass spectrum of HNF.

method developed by Frankel et. al [11,12]. Subsequently HNF of high purity was obtained by neutralization of NF with hydrazine hydrate [13] and was given special treatment for obtaining it in free-flow form [14].

Recrystallized HNF in MeOH/CTC yielded yellow needle-shaped particles: mp, 120°C; purity >98% (HPLC); anal. calcd. for $CH_5N_5O_6$: C, 6.55: H, 2.75: N, 38.25: O, 52.45, Found: C, 6.66: H, 2.73: N, 38.03: O, 52.58; UV spectra (H_2O): λ_{max} 210, 352 nm; IR spectra (KBr matrix): N-H str: 3244 cm^{-1} (m), NH_3^+ def: 1615 cm^{-1} (w), NO_2 asy. str: 1512 cm^{-1} (s), NH_3^+ bend: 1420 cm^{-1} (m), NO_2 sy. str: 1271 cm^{-1} (s), NH_3^+ wag: 1180 cm^{-1} (s), N-C-N asy. str: 1100 cm^{-1} (m), NO_2 bend: 790 cm^{-1} (s), N-N str: 971 cm^{-1} (m); ^{1}H NMR spectra (300 MHz, DMSO-d_6):δ7.028 (s, 5H); ^{13}C NMR spectra (300 MHz, DMSO-d_6): δ 150.759 (w, 1C); MS m/z calcd. for NH_4-C-$(NO_2)_3$: 168, C-$(NO_2)_3$: 150, NH_4-C-$(NO_2)_2$: 122, HC-$(NO_2)_2$:105, $NH_4NO_3.H_2O$ 98, NH_4NO_3: 80. Found NH_4-C-$(NO_2)_3$: 168 (30%), C-$(NO_2)_3$: 149 (100%), NH_4-C-$(NO_2)_2$: 122 (18.6%), HC-$(NO_2)_2$: 105 (16.5%), $NH_4NO_3.H_2O$: 97 (9.5%), NH_4NO_3: 81 (11.4%).

UV and IR spectra match with the reported data. In ^{1}H NMR spectra the expected multiplets are not observed because of

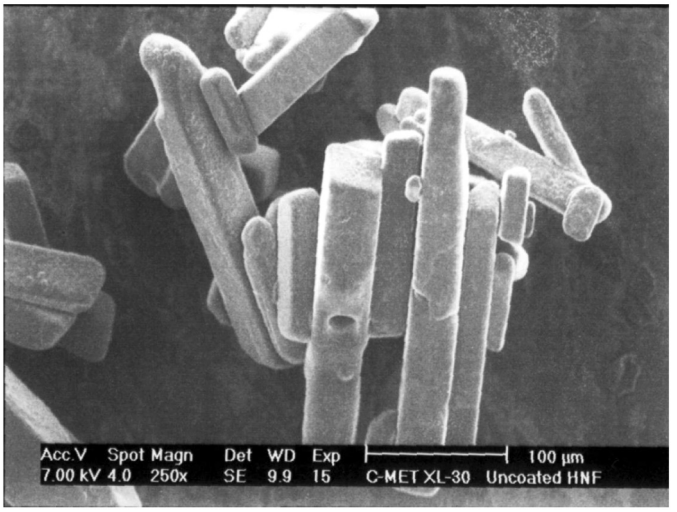

Figure 2. SEM of needle-shaped HNF crystals with 250 × magnification.

Table 1
XRD data of HNF

d value (Å)	Relative intensity	d value (Å)	Relative intensity	d value (Å)	Relative intensity	d value (Å)	Relative Intensity
21.6928	27.7%	3.9362	43.0%	2.6338	36.9%	2.0371	9.2%
9.6623	21.7	3.8512	23.0	2.6115	49.1	1.9724	13.3
9.3265	61.7	3.7003	13.6	2.6019	26.4	1.8061	4.6
9.2053	36.4	3.6502	22.4	2.5177	18.8	1.7471	3.3
7.9431	4.1	3.6166	64.9	2.5060	36.4	1.7332	5.1
6.3363	8.0	3.5843	37.9	2.4964	31.7	1.6963	14.2
6.0633	26.0	3.4848	10.5	2.4496	4.4	1.6738	9.2
5.5955	16.4	3.3620	37.9	2.4007	17.1	1.6447	6.3
5.5381	11.6	3.3074	20.2	2.3735	41.4	1.5443	4.1
5.3941	3.9	3.0426	84.5	2.3039	35.4	1.4481	0.8
4.7946	32.1	3.0204	100	2.2988	42.5	1.4008	1.7
4.7576	28.6	2.9873	87.5	2.2859	39.9	1.3693	2.9
4.6585	16.4	2.9011	11.8	2.2792	32.1	1.3153	2.6
4.6093	26.0	2.8233	34.0	2.2646	37.4	1.2763	1.9
4.5519	49.6	2.8061	46.8	2.2200	13.3	1.2544	2.6
4.3903	21.7	2.7680	40.9	2.2010	11.8	1.2359	1.7
4.3215	75.6	2.7436	71.6	2.0895	3.0		
4.2610	57.9	2.6939	34.9	2.0652	5.7		

intermolecular exchange of hydrogen on nitrogen atoms. In ^{13}C NMR spectra, the intensity of peak was very weak, though the spectra was run for a large number of pulses (2500) with long interval (1.0 μsec). This may be due to the presence of a quaternary carbon atom in the compound. In mass spectra (Figure 1) the parent N_2H_5-C-$(NO_2)_3$ molecule (m/e,168) does not appear because of its decomposition prior to vaporization [15].

3.2 Crystallographic Study of HNF

SEM of HNF revealed layers of needle-shaped crystals with varying L/D ratios (Figure 2). The d values obtained from XRD pattern (Table 1, Figure 3) bring out the monoclinic nature of the HNF crystal as reported [7,16]. This was supported by theoretical calculations of

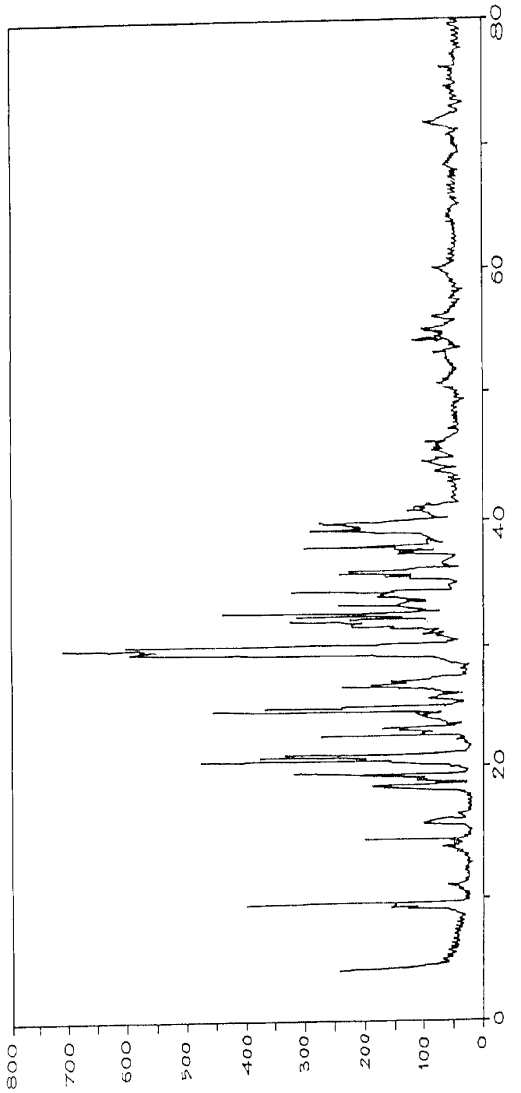

Figure 3. XRD spectrum of HNF.

interplanar spacing applicable to the monoclinic crystal system [5] by the equation

$$d_{hkl} = \frac{1}{\left[\frac{h^2/a^2 + l^2/c^2 \div 2hl\cos\beta/ac}{\sin^2\beta} + k^2/b^2\right]^{\frac{1}{2}}}$$

where $a = 7.91\,\text{Å}$, $b = 11.77\,\text{Å}$, $c = 13.98\,\text{Å}$, and $\beta = 104^\circ$.

TEM spectrometry also suggests the monoclinic nature of HNF (Table 2).

The XPS spectra peaks of HNF were broad and asymmetric toward the higher-energy side. The C1s spectrum with full width at half maxima (FWHM: 4.2 eV) was resolved into four Gaussion peaks (Figure 4). After subtracting the background by the Shirley background method, binding energies (BEs) of the corresponding peaks are found to be 285, 286.2, 289, and 291.2 eV respectively. The first peak with BE of 285 eV is attributable to the strong $C^{\delta-}-H\text{-}N^{\delta+}$ intermolecular hydrogen bonding between nitroformate and hydrazinium ions [16]. The second peak with a BE of 286.2 eV is assignable to the C-N bond. The third and fourth peaks may be due to polar interaction between HNF molecules. However, their exact assignment needs detailed investigation.

The N1s spectrum (FWHM: 3.6 eV) was resolved into three Gaussian peaks. After subtracting the background (Figure 5), BEs of the respective peaks correspond to 398, 399.4, and 401.8, eV respectively. These peaks are assignable to C-N, -NH_2, and -NO_2 bonding, respectively.

Table 2
TEM data of HNF

d Value (Å)	Relative intensity
3.114	100%
3.655	64
5.686	16
6.567	8
8.733	5

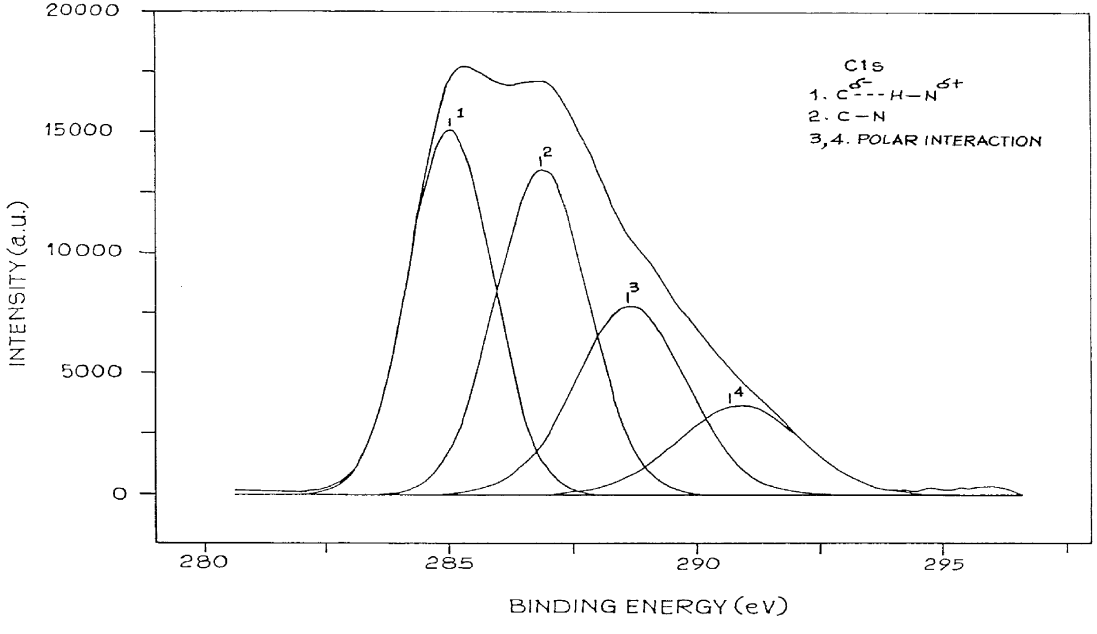

Figure 4. XPS Curve of HMF.

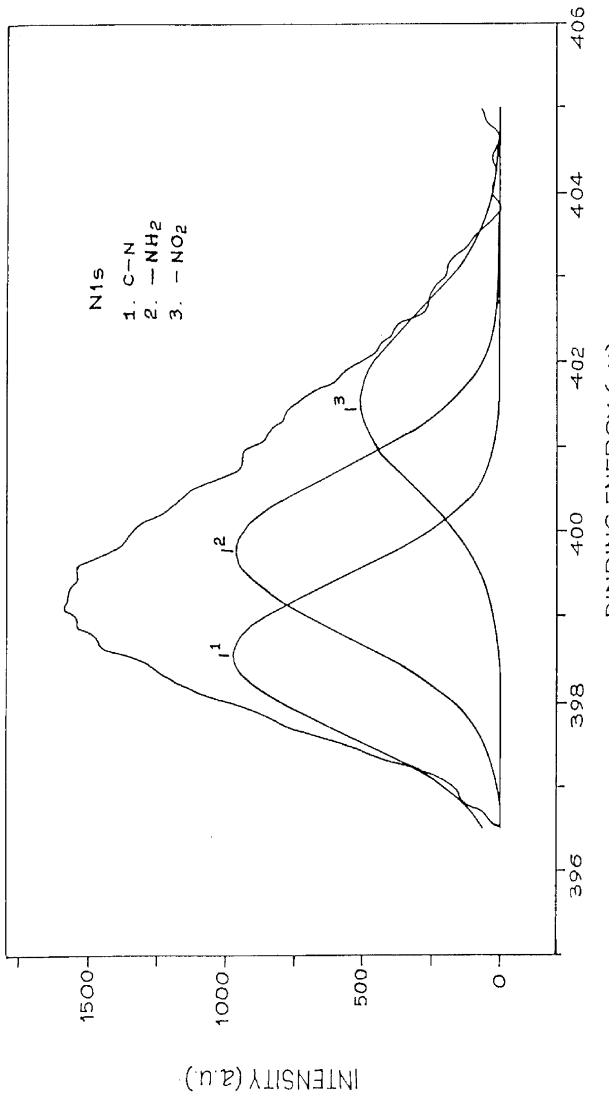

Figure 5. XPS Curve of HNF.

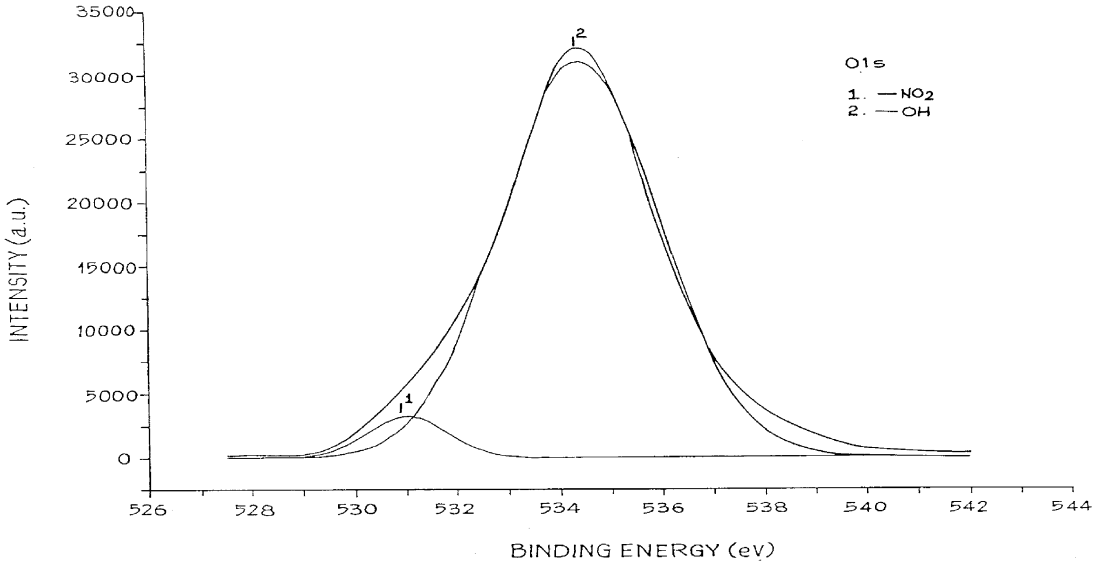

Figure 6. XPS Curve of HNF.

The O1s spectrum (Figure 6) was resolved into two peaks with BEs of 531 and 534 eV. The first peak may be due to oxygen from NO_2 species, while the other peak may be because of the adsorbed -OH species on the surface of HNF crystals or hydrogen bonding between oxygen of one HNF[-C $(NO_2)_3]^-$ ion through the H of the $N_2H_5^+$ ion of the neighboring HNF [16]. The high peak area of the latter peak (as compared to the former) may be due to the high magnitude of strong hydrogen bonding on the surface.

The DSC (Table 3, Figure 7) are curve exhibited two exotherms with maximum temperature of decomposition (T_{max}) at ~136 and 138°C, respectively. The energy of activation obtained from the data generated at different heating rates by the Kissinger method [8] for the first and second exotherm was 150 kJ/mol with a pre-exponential factor of 1.3×10^{19} and 1.5×10^{19}, respectively. The Ozawa method [9] gave a similar value ($E = 149$ kJ/mol). DTA and TG studies also revealed two-stage decomposition of HNF (Table4; Figure 8). In TG the first-stage decomposition (temperature range: 105–142°C) showed 72.5% weight loss, whereas in the second stage of decomposition (temperature range: 142–210°C) the weight loss was 24.5%.

Decomposition temperatures of exotherms obtained during the present work are in close agreement with the data reported by Schoyer et al. [1,4,17]. Koroban et al. [15] have reported formation of ANF as an intermediate during slow decomposition of HNF. Williams and Brill [17] have suggested decomposition of ANF to AN. The activation

Table 3
DSC results of HNF at different heating rates

	First exotherm			Second exotherm			
Heating rate (°C/min)	T_i (°C)	T_{max} (°C)	T_f (°C)	T_i (°C)	T_{max} (°C)	T_f (°C)	ΔH (J/g)
5	127.6	130.2	132.3	132.3	133.3	176.7	−2301
10	131.9	135.8	137.9	137.9	138.2	178.3	−2676
15	134.2	139.8	142.1	142.1	143.6	192.2	−2389
20	135.6	142.1	144.2	144.2	145.1	190.8	−2954
25	137.2	144.7	146.5	146.5	147.9	200.2	−2535

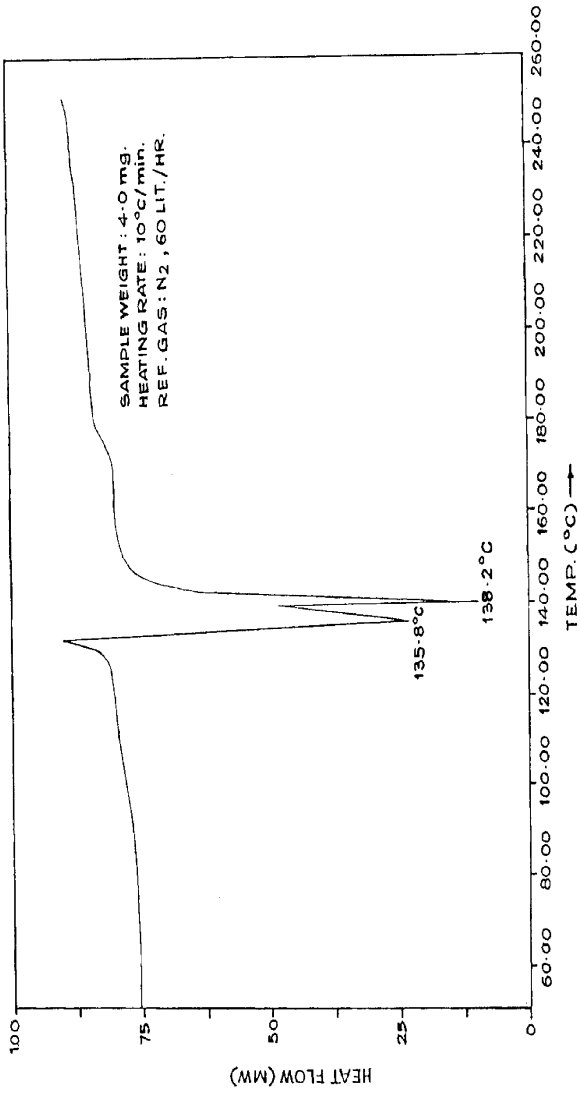

Figure 7. DSC Curve of HNF.

Table 4
DTA/TG results of HNF

	DTA			TG		
Peak details	T_i (°C)	T_{max} (°C)	T_f (°C)	Stages of decomposition	Temperature range (°C)	Loss in weight
First exotherm	130.7	133.5	135.5	First stage	105–142	72.5%
Second exotherm	135.5	137	171.2	Second stage	142–210	24.5

energy obtained in DSC experiments for the first exotherm is close to that reported by Williams and Brill. The weight loss trend obtained during this work suggests formation of the cyanamide-type species, which might have resulted from rapid decomposition of HNF and recombination of decomposed species. To get additional evidence, HNF was also subjected to thermal decomposition in a hyphenated TG-FTIR system (Figure 9). The IR spectrum of the decomposed products revealed the presence of moieties containing the –C≡N group, which might have resulted from decomposition of cyanamide-type species. Nitro and amino species were also detected in the decomposed gases.

4. Conclusion

The present study shows that HNF of desired purity and morphology can be obtained by optimizing the process. Elemental analysis and spectroscopic methods confirmed the structural features of HNF synthesized in this laboratory. TEM spectroscopy supported the monoclinic structure of HNF as interpreted from XRD data. XPS spectra suggest strong inter-molecular hydrogen bonding between HNF molecules.

Thermal studies reveal two-stage decomposition of HNF, subsequent to the melting with the activation energy of 150 kJ/mol. Weight loss pattern and TG-FTIR studies are indicative of the formation of cyanamide-type species during thermal decomposition.

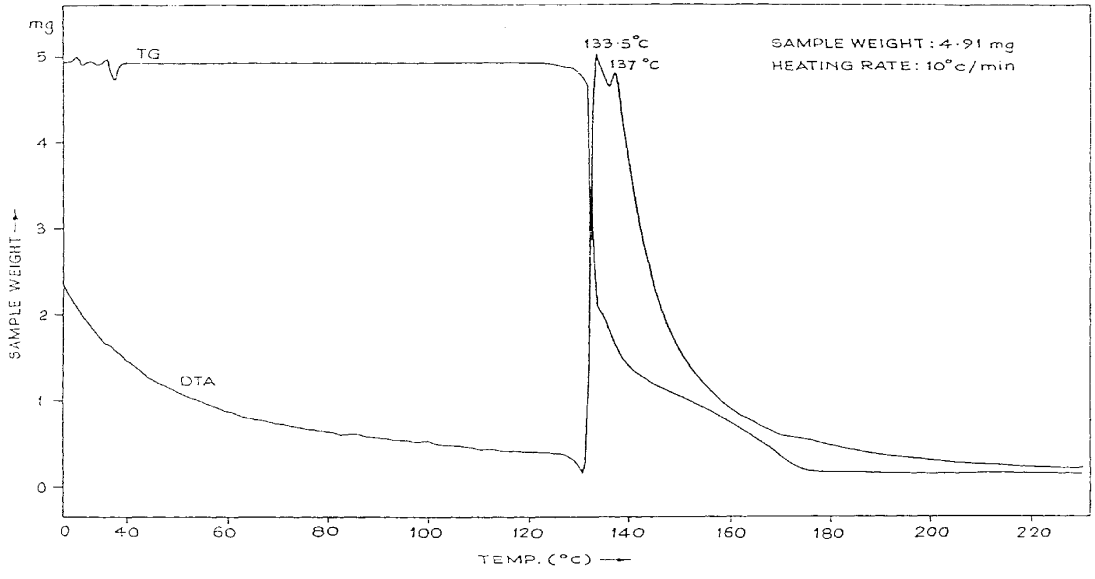

Figure 8. DTA/TG Curve of HNF.

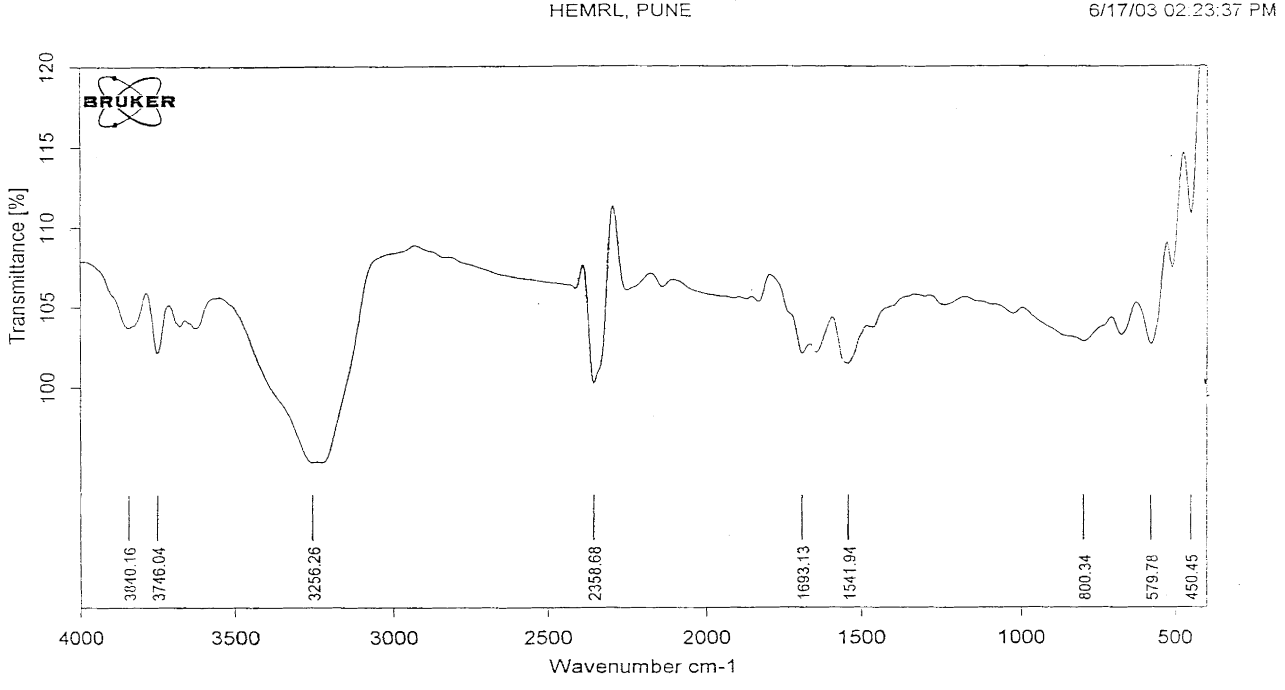

Figure 9. TG-FTIR Spectrum of HNF.

References

[1] Schoyer, H. F. R., Schnorhk, A. J., Korting, P. A. O. G., Van Lit, P. J., Mul, J. M., Gadiot, G. M. H. J. L., and Meulenbrugge, J. J. 1995. *J. Propul. Power* 11(4):856.
[2] Louwers, J. 1997. *J. Pyrotech.* 6:36.
[3] Meulenbrugge, J., Steen, A. V. D., and Hyden, A. V. D. 1995. *Proceedings of International Symposium of Energetic Materials & Technology*, Arizona, pp. 297–302.
[4] Hideo, H., Toshio, O., Seiichi, K., and Shigeru, S. 1994. *Proceedings of 20th International Pyrotechnic Seminar & Conference*, Chicago, pp. 397–402.
[5] McLachlan, D., Jr. 1967. in *Hand book of X-rays*, ed. E. F. Kaelble, New York: McGraw Hill, p. 4/1.
[6] Hordijk, A. C., Mul, J. M., Meulenbrugge, J. J., Korting, P. A. O. G., Van Lit, P. L., Schnorhk, A. J., and Schoyer, H. F. R. 1994. *Proceedings of 25th International Annual Conference of ICT*, Karlsruhe, Germany, 69/1-69/11.
[7] Schoyer, H. F. R., Schnorhk, A. J., Korting, P. A. O. G., and Van Lit, P. J. 1997. First experimental results of an HNF/Al/GAP solid propellant, AIAA paper No. 97–3131.
[8] Kissinger, H. E. 1957. *Anal. Chem.* 29:1702.
[9] Ozawa, T. 1965. *Bull. Chem. Soc.* 38:1881.
[10] Frankel, M. B., Gunderloy, F. C., and Woolery, D. O., II. 1978. US Patent 4,122,124.
[11] Frankel, M. B., Raniere, F. D., Thompson, W. W., Witucki, E. F., and Woolery, D. O., II. 1979. US Patent 4,147,371.
[12] Frankel, M. B., Bauerle, G. L., Grant, L. R., Kistner, R. L., Lecce, J. V., Wilson, E. R., and Woolery, D. O., II. 1987. Final Report No. UCRL-15908, DE87 012924, Rockwell International, California, pp. 1–57.
[13] Lovett, J. R., and Edison, N. J. 1968. US Patent 3,378,594.
[14] Dendage, P. S., Sarwade, D. B., Asthana, S. N., and Singh, H. 2001. Indian patent applied.
[15] Koroban, V. A., Smirnova, T. I., Barishova, T. N., and Svetlov, B. S. 1979. Tr.- Mosk. Khim.-Tekhnol. Inst., D.I. Mendeleeva, 104:38.
[16] Dendage, P. S., Sarwade, D. B., Asthana, S. N., and Singh, H. 2001. *J. Energ. Mater.* 19(1):41.
[17] Milicev, S., and Macek, J. 1986. *J. Spectrochem. Acta.* 41A:651.
[18] Bellerby, J. M., Backman, C. S., Van Zelst, M., and Van der Heijden, A. E. D. M. 2000. *Proceedings of 31st International Annual Conference of ICT*, Karlsruhe, Germany, pp. 104/1–104/15.
[19] Dickens, B. 1970. *J. Res. Natl. Bureau Stds.* 74A:309.
[20] Williams, G. K., and Brill, T. B., 1995. *Combust. Flame* 102(3):418.